Journal of the Korean Physical Society, Vol. 49, No. 1, July 2006, pp. 370∼375

Designing Points of a Single-Particle Mass Spectrometer in Terms of Aerosol Focusing and Ion Loss

Donggeun Lee,* Sung-Woo Cho, Seung Geun Lee and Sang-Gyu Kim
School of Mechanical Engineering, Pusan National University, Busan 609-735

(Received 25 January 2006)

In this article, we raise several important concerns which should be considered for the development of a single-particle mass spectrometer (SPMS). They are related to the performance and the characteristics of the components of that machine, *i.e.*, aerosol collimation, laser ionization, and ion kinetic effects. We attempted to address those concerns through visualizations of the aerosol beam with light scattering, molecular dynamics simulations to elucidate the mechanism for energetic-ion formation, and a new conceptual design of ion optics. As such, we offer guidance for the development of a SPMS that will be capable of simultaneously analyzing the size and the elemental composition of a single nanoparticle.

PACS numbers: 82.70.R
Keywords: Single particle mass spectrometer, Nanoparticle, Composition, Size

I. INTRODUCTION

Together with increasing interest in nanoparticle technology including novel synthesis and applications of particles, an ideal tool capable of characterizing physical and chemical phenomena occurring at the nanoparticle level is required more and more every year because single-particle analysis directly gives an insight into what happens inside the particle during the synthesis or reaction [1]. Single-particle mass spectroscopy (SPMS) may be the closest candidate to an ideal tool. Conventional SPMS, described elsewhere [2], has been used historically for characterization of coarse-mode particles (>200 nm) in the environment. The SPMS has been called differently as aerosol mass spectroscopy (AMS) or laser desorption-ionization mass spectroscopy (LDIMS). As AMS or LDIMS employs light scattering for sizing particles, as well as triggering the ionizing laser, the measurable size of particles is limited to sizes larger than 200 nm. This has hindered the use of that machine to the accumulation- or nuclei-mode particles that are more important in a study of health effects in environment technology. Also, the power of a conventional laser installed on the AMS may appear to be insufficient for complete ionization of a particle because the mass spectra consist of only positive and negative molecular ions. The different polarities of such ions facilitate rapid recombination and charge transfer from ions with larger ionization potentials (IP) to those with less IP [1]. This yields some bias in the composition of the particle. For this reason, the majority of research has reported qualitative, rather than quantitative, assignment of the elements composing an environmental particle rather than quantification.

More recently, we proposed the possibility of using a much stronger laser pulse seemed to solve the problem of insufficient laser power as a high-power laser pulse tears a particle into its constituent atoms and subsequently ionize them. If the beam energy is strong enough to take an electron out of the components with a high electron affinity, we will observe only positive-ion mass spectra. As positive ions are not likely to collide with each other frequently, we may avoid charge transfer. Reents and Ge [3] claimed that the observation of multiply charged ion peaks might be the sign of such a case and showed that the stoichiometric ratio got closer to the theoretical value. As we observed the same thing and affirmed complete ionization, we thought the sum of the signal intensities in the mass spectrum should be proportional to total number of atoms (volume) of a particle, but we saw that the former increased with a half power of the latter. The nonlinearity was attributed to size-dependent ion losses while they traveled from the laser focus to the detecting position. With the correlation between mass spectrum and the particle size, we eventually mimicked the size distribution of particles nicely [4].

We demonstrated that a SPMS with the capability of simultaneously measuring the sizes and the compositions of particles could be used to elucidate various nanoscale phenomena, for example, the solid-state reaction kinetics inside a nanoparticle [1], size-resolved surface reaction kinetics [5], and the origins of environmental particles [6]. Hence, the usefulness of the SPMS is obvious. However, we point out here that the key correlation, the so-

*E-mail: donglee@pusan.ac.kr; Fax: +82-51-512-5236

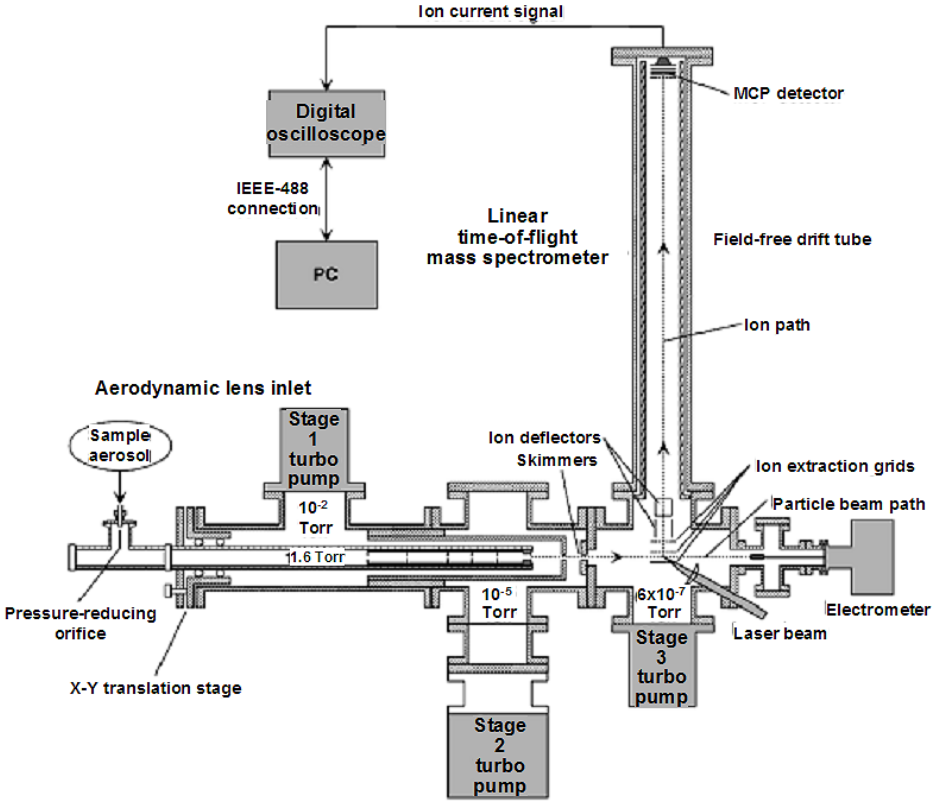

Fig. 1. Schematic of a single-particle mass spectrometer.

called power-law relationship, basically requires another assumption that the kinetic effect of positive ions (confirmed by ion tracing [4]) be size-dependent. We still need to evaluate the adequacy of that assumption. In this research, we employed a molecular dynamics simulations to explore the nature of energetic-ion formation. Also, we not only raise some important design points necessary for the development of the advanced SPMS, but also address them.

II. EXPERIMENT

Our single-particle mass spectrometer consists of an aerodynamic inlet, a source region for particle-to-ion conversion with a free firing high powered Nd:YAG laser, a linear time-of-flight (TOF) tube, and a multichannel plate detector (MCP), as shown in Fig. 1. An aerodynamic lens inlet is employed to separate particles from the carrier gas and collimate them so that they can be injected without traveling losses through differentially pumped chambers to the ionization region. As configured, the positive ions formed from a particle by multiphoton laser ionization are accelerated along the ∼1-m-long linear TOF tube and are detected with the MCP. Fig. 2 shows an example of the mass spectrum of a NaCl nanoparticle generated by spray drying. A more detailed

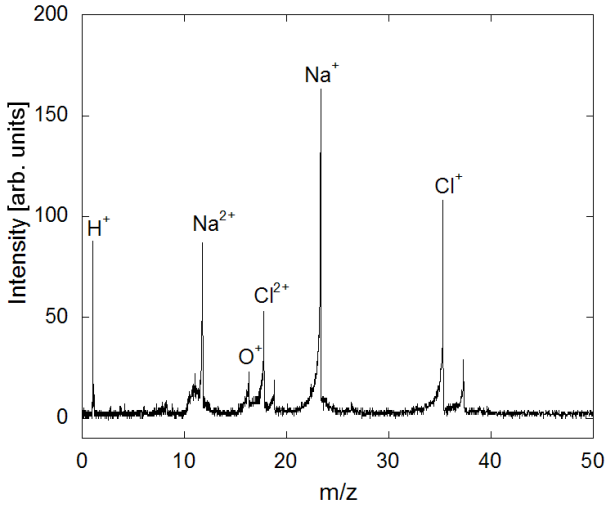

Fig. 2. Mass spectrum of a single NaCl particle.

explanation of the instrumentation and nanoparticle generation is given elsewhere [1].

III. DESIGN POINTS

There are two design points for development of the advanced SPMS. The first is, as expected, related to aero-

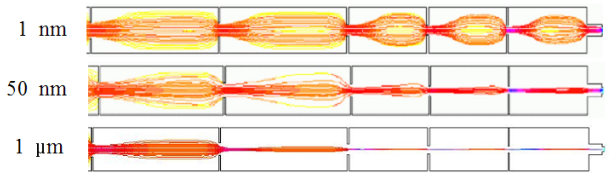

Fig. 3. Simulations of particle trajectories.

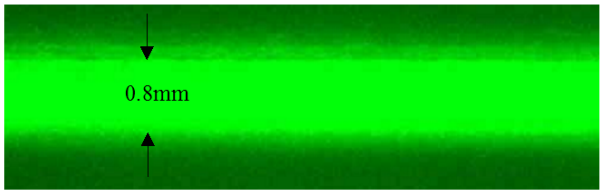

Fig. 4. Photograph of a particle beam.

dynamic lens inlet for focusing aerosols, and the second is how to prevent ion loss.

1. Aerosol Focusing with an Aerodynamic Lens

As the particles are focused tightly more and more, we get more chance for the laser pulse to hit the particles. This is very important, especially for studying environment aerosols, because the current hitting efficiency is not sufficient for dilute samples ($<10^4$ #/cc). Thus, we have been attempting to increase the focusing performance by testing several designs of the lens. As a first step, we simulated the aerosol trajectories with Fluent and confirmed that the aerosol particles are indeed focused as seen in Fig. 3. The smallest particles with diameters of 1 nm show gas-like behavior, *i.e.*, expansion and contraction before and after each orifice, which is due to their light mass, whereas the heavier particles deviate from the gas stream line, begin to move toward the centerline, and eventually form a very narrow particle beam. The contraction ratio of an aerosol beam with respect to the inner diameter of the original tube improves from 5.7 % to 0.8 % (1.5 mm to 0.2 mm) as the tested particle size increases from 1 nm to 1 μm, respectively. It is notable that the heavy particles are tugged to the orifice walls due to excessive inertia. When the transmission efficiency (TE) of particles is defined as the ratio of the number of particles before entering the whole lens to that of particles passing through the final nozzle, we find that the TE decreases from 95 % to 56 % when the particle size increases from 1 nm to 1 μm. One may predict the particle-size distribution from the frequency at each bin of signal intensities in a set of analyzed data. But one has to take into account the size-dependent TE prior to doing so. In other words, one should correct some bias of the distribution toward larger sizes by dividing the frequency by the corresponding TE. The ideal inlet should focus all differently sized particles with no loss. Note that the simulation was made without consideration of particle diffusion.

To verify the focusing performance, we used light scattering to visualize the aerosol beam. Fig. 4 obviously shows that the aerosol beam is quite tightly focused. The beam of small particles is broaden at 22 cm downstream of the inlet end while larger particles are more collimated at the same position, but with greater loss. The measured aerosol beam diameter is 0.8 mm, which lies reasonably within the predicted range (0.2∼1.5 mm). Note that as the predictions were made without consideration of Brownian diffusion of particles [7], the simulation should give a lower limit on the beam diameter. Also, regarding the strong size-dependency of the scattered light intensity, the visualization should be dominated by larger particles. That is why the aerosol beam is a little bit larger than the prediction. In the future, we will attempt to reduce the beam size more by using electrical charging and an Einzel lens.

2. Origin of the Kinetic Effects of Positive Ions

As addressed shortly in the Introduction, we raised, for the first time, the size-dependent ion loss being mainly due to the size-dependency of energetic-ion formation [4]. In this section, a molecular dynamic simulation is used to figure out what happened. We postulate that positive ions generated by a nanosecond high-power laser pulse form a spherical ion cloud, which has often been adopted for the breathing sphere model [8]. The spherically symmetric system makes the calculation much simple.

It has been observed that very energetic positive ions up to 1 MeV are formed when a femto-second laser pulse deposits a gas cluster [8,9]. The dynamics and maximum kinetic energy of the ions were predicted qualitatively well by Ditmire *et al.*'s nanoplasma model [8]. Note that the femto-second laser pulse had an extremely large intensity ($>10^{15}$ W/cm^2 at least), which implies that, even at the beginning of the pulse, enough electrons exist for collisional ionization in a spherical plasma cloud. Collision ionization increases the electron density rapidly, often up to more than critical value. The highly dense electrons in a nanoplasma ball are heated resonantly by the surrounding laser field, leading to a very rapid expansion of the plasma ball. Tunneling, collision-induced ionization, and subsequent nanoplasma resonance with the pulse seem very likely to be accepted by the research community.

In contrast, the majority of nanosecond lasers used for the SPMS have a much lower intensity, typically less than 10^{10} W/cm^2. This intensity seems to be insufficient to supply electrons via particle ionization to such a high density. Therefore, resonance heating of the plasma ball may not occurs, in turn, the above-mentioned hydrodynamic expansion may not be the case.

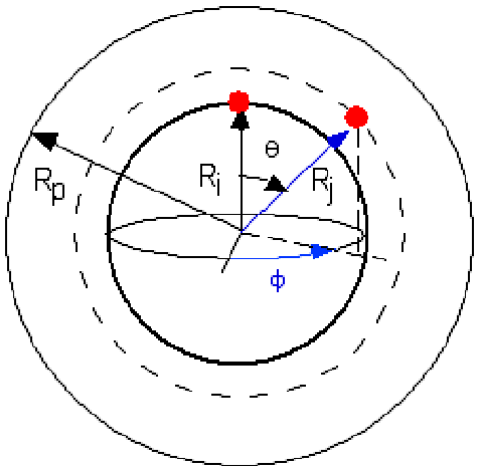

Fig. 5. Spherical coordinate system for an ion cloud.

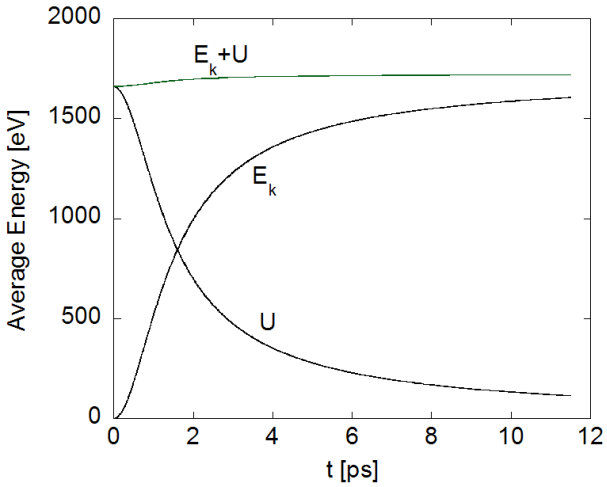

Fig. 6. Total energy conservation during the molecular dynamic simulation.

Indeed, single-photon or multi-photon ionization of clusters or gas molecules with nanosecond laser pulse at low-to-moderate intensities has been studied, and the photofragmentation [10] and Coulomb explosion [11] dynamics have been proposed as the corresponding mechanism. The kinetic energy (KE) of the ions at those intensities was revealed to be much less than in the former case.

Together with contradictions in the mechanism, whether the cluster can be treated as a plasma or not has given rise to a controversy. For example, classical dynamics simulations including the Coulomb field of the ions indicate that the electrons are quickly removed at the beginning of the interaction even from large clusters [12]. That makes the nanoplasma model [8] questionable. Note that all the above discussions are only for gas clusters, not nanoparticles. There are no available experimental data for nanoparticles. Are we between a nanoplasma ball and a positive ion cloud, or hydrodynamic and Coulombic expansion? Unfortunately, we are not currently in a position to answer that question. Regarding our conditions, for ionization of a nanoparticle by a long (5 ns) much weaker ($\sim 10^{10}$ W/cm^2) laser pulse, the condition should lie between the above two cases and seems likely to be closer to the Coulombic expansion.

We, therefore, choose the simplest model, the main assumption of which is as follows. Particles are completely ionized [4] to yield positive ions which form a spherical cloud. The interaction of each pair of ions is depicted by Coulomb repulsion. Fig. 5 shows the coordinate system. In the figure, R_i and R_j denote the radial position vectors of the i^{th} and the j^{th} ions. First, we derive the force vector exerted on the i^{th} ion by the j^{th} ion by differentiating the corresponding Coulombic potential; then, the total potential of i by all j ions is given by

$$U_i = \frac{1}{4\pi\epsilon_0}\int\int\int \frac{\rho^2 V_0}{r_{ij}} r_j^2 \sin\theta_j d\theta_j d\phi_j dr_j$$

$$= \frac{\rho^2 V_0}{12\epsilon_0}(3R^2 - r_i^2) \quad (1)$$

The total potential energy of the cloud is obtained by integrating the above U_i:

$$U = \int\int\int U_i 4\pi r_i^2 dr_i = \frac{4}{15}\frac{\pi}{\epsilon_0}\rho^2 R^5,$$

$$\bar{U} = \frac{U}{N_s} = \frac{Ue}{\rho\frac{4}{3}\pi R^3} = \frac{\rho R^2}{5\epsilon_0} \quad (2)$$

This is the first explicit expression for the size dependency of the potential energy of ions. The potential energy is completely converted into kinetic energy after sufficient time, which is confirmed in Fig. 6. The equation obviously shows that a larger particle or ion cloud leads to a higher potential and kinetic energy. The mean kinetic energy of the ions (the second equation in Eq. (2)) is proportional to the surface area of the original particle. Surprisingly, the previous experiment showed a 1.6^{th} power for the R dependence, which was pretty close to the second power of R in Eq. (2). That proximity supports our model that the energetic ion may form through Coulombic repulsion. Eventually, we obtain the radial distribution of ion kinetic energy, as well as force on and velocity of the ions. Ions at the surface move fastest due to the largest repulsion potentials. Those ions will be detected with the lowest efficiency, resulting in an underestimate of the surface atoms. This implies that if core-shell-shaped particles are of interest, the measured composition can be biased toward the core. To prevent this, we need to design new kinetic-energy-independent ion optics.

3. Development of Ion-loss-free Ion Optics

The conventional ion optics in the source region consist of one repelling plate, two flat grids, and two pairs of

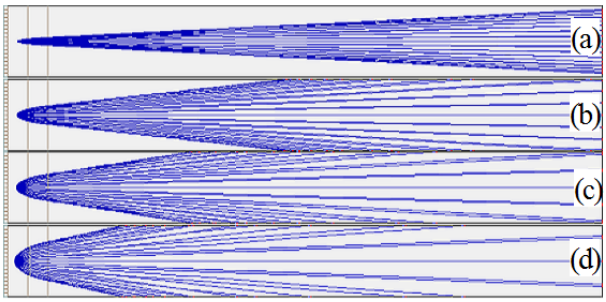

Fig. 7. Ion trajectories at different kinetic energies of the ions: (a) 10 eV, (b) 50 eV, (c) 100 eV, and (d) 200 eV.

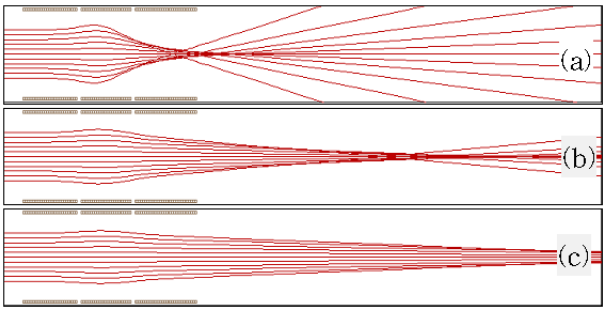

Fig. 8. Ion focusing with an Einzel lens: (a) 100 eV, (b) 150 eV, and (c) 200 eV.

ion-manipulating plates, as seen in Fig. 1. The ion manipulators are not often used. Fig. 7 shows typical ion trajectories in the present design of the SPMS. As the kinetic energy increases, the ions are moving outward from the centerline of the TOF tube, implying such ions are terminated at the inner wall of the tube and not detected. According to the molecular dynamics simulation results, ion loss from larger particles gets bigger. Intuitively, we are aware that diverging ion trajectories are compressed more if the configuration of the repelling plate is bent like s concave plane. We confirmed that ions trajectories become more compressed as the curvature of the plate is increased.

Secondly, we employ an Einzel lens consisting of three cylindrical tubes, as seen in Fig. 8. The first and the third tubes are electrically grounded while the central tube, which is equidistant from the first and the third ones, is held at a positive voltage (500 V in the simulation for Fig. 8). The incident ions are first decelerated and then accelerated. At the same time, they begin to move to the centerline of the TOF tube. Thus, the ion beam can be focused by using this lens system without imparting any net acceleration to the ions. However, note that the extent of focusing depends on the initial kinetic energy of the incident ions. Ions moving slower are even overfocused. Also note that the performance of the Einzel lens becomes maximized for ions that are parallel with the tube's center line. If the ions are approaching the centerline at an angle, the overfocusing becomes worse at the same speed. There is no voltage

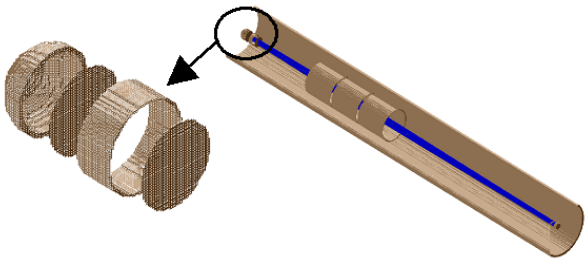

Fig. 9. Optimum design of ion optics displayed with a TOF tube.

condition for which all ions are focused uniformly.

We notice that for better performance, the ion trajectories should be parallel to the axis of the Einzel lens before entering the lens. As ions moving away from the repelling plates are radially diverging, a series of the two elements are used together, as seen in Fig. 9. All ions with kinetic energies of 0 to 200 eV are successfully converged to the MCP detector. This means that the new SPMS is the only one that guarantees 100 % detection efficiency of ions with no ion loss over a wide range of kinetic energies [13].

IV. CONCLUSIONS

In this paper, we pointed out two design points which should be kept in mind for design of a novel single-particle mass spectrometer. Theoretical and experimental results for the aerodynamic lens inlet showed that the inlet was able to collimate aerosol nanoparticles and form a tightly focused aerosol beam. Also, using a molecular dynamics simulation, we asserted that energetic ion formation caused by a nanosecond high-power laser pulse was primarily due to Coulombic repulsion of positive ions. Finally, for ions optics, we proposed a new design concept that is capable of 100 % detection of ions having a wide range of kinetic energies.

ACKNOWLEDGMENTS

This work was supported by the Core Environmental Technology Development Project for Next Generation (Project No. 102-041-029).

REFERENCES

[1] R. Mahadevan, D. Lee, H. Sakurai and M.R. Zachariah, J. Phys. Chem. A **106**, 11083 (2002).
[2] C. A. Noble and K. A. Prather, Mass Spectrom. Rev. **19**, 248 (2000).

[3] W. D. Reents and Z. Ge, Aerosol Sci. Tech. **33**, 122 (2000).
[4] D. Lee, K. Park and M. R. Zachariah, Aerosol Sci. Technol. **39**, 162 (2005).
[5] K. Park, D. Lee, A. Rai, D. Mckherjee and M. R. Zachariah, J. Phys. Chem. B **109**, 7290 (2005).
[6] D. Lee, A. Miller, D. Kittelson and M. R. Zachariah, J. Aerosol Sci. **37**, 88 (2005).
[7] B. Liu, P. L. Ziemann, D. B. Kittelson and P. H. McMurry, Aerosol Sci. Technol. **22**, 293 (1995).
[8] T. Ditmire, T. Donnelly, A. M. Rubenchik, R. W. Falcone and M. D. Perry, Phys. Rev. A **53**, 3379 (1996); J.-S. Yoon, T. Lho, Y. H. Jung, B. Lee, S.-J. Yoo and S.-H. Lee, J. Korean Phys. Soc. **46**, 855 (2005); K. S. Hong and H.-S. Yang, J. Korean Phys. Soc. **47**, 200 (2005).
[9] M. H. R. Hutchinson, T. Ditmire, E. Springate, J. W. G. Tisch, Y. L. Shao, M. B. Mason, N. Hay and J. P. Marangos, Phil. Trans. R. Soc. Lond. A **356**, 297 (1998).
[10] Z. Y. Chen, C. D. Cogley, J. H. Hendricks, B. D. May and A. W. Castleman, J. Chem. Phys. **93**, 3215 (1990).
[11] J. T. Snodgrass, C. M. Roehl and M. T. Bowers, Chem. Phys. Lett. **159**, 10 (1989).
[12] I. Last and J. Jortner, J. Phys. Chem. A **102**, 9655 (1998).
[13] D. Lee and S.-W. Cho, *Single-Particle Mass Spectrometer* (Korean Patent Applications, 2005).